INL/CON-16-37798
PREPRINT

Modelling of LOCA Tests with the BISON Fuel Performance Code

Enlarged Halden Programme Group Meeting

R. L. Williamson, G. Pastore, S. R. Novascone,
B. W. Spencer, J. D. Hales

May 2016

The INL is a
U.S. Department of Energy
National Laboratory
operated by
Battelle Energy Alliance

Modelling of LOCA Tests with the BISON Fuel Performance Code

G. Pastore, R.L. Williamson, S.R. Novascone, B.W. Spencer, J.D. Hales*
Fuel Modeling and Simulation, Idaho National Laboratory, Idaho Falls, United States
**Giovanni.Pastore@inl.gov*

Abstract

BISON is a modern finite-element based, multidimensional nuclear fuel performance code that is under development at Idaho National Laboratory (USA). Recent advances in BISON include the extension of the code to the analysis of LWR fuel rod behaviour during loss-of-coolant accidents (LOCAs). In this work, BISON models for the phenomena relevant to LWR cladding behaviour during LOCAs are described, followed by presentation of results from simulations of LOCA tests. Analysed experiments include separate effects tests of cladding ballooning and burst, as well as the Halden IFA-650.2 fuel rod test. Two-dimensional modelling of the experiments is performed, and calculations are compared to available experimental data. Comparisons include cladding burst temperature, pressure and time for separate effects tests, as well as the evolution of fuel rod inner pressure during ballooning and time to cladding burst for IFA-650.2. Furthermore, BISON three-dimensional simulations of separate effects tests are performed, which demonstrate the capability to reproduce the effect of azimuthal temperature variations in the cladding. The work has been carried out in the framework of the collaboration between Idaho National Laboratory and Halden Reactor Project, and of the IAEA Coordinated Research Project FUMAC.

1. Introduction

Developing state-of-the-art computational tools for reliably predicting the thermo-mechanical behaviour and integrity of the nuclear fuel rods in light water reactors (LWRs) during accidents is essential from both safety and economic standpoints. For this purpose, increasingly complex and efficient fuel performance codes [1,2] are developed. Also, fuel performance codes able to simulate accident conditions can be used to aid the development of accident-tolerant fuel concepts [3,4].

BISON [5] is a modern finite-element based, multidimensional fuel performance code that has been under development at Idaho National Laboratory (INL, USA) since 2009. The code is applicable to both steady and transient fuel behaviour and can be used to analyse 1D, 2D axisymmetric and cartesian, or 3D geometries. Although primarily used for LWR fuel analysis, BISON has been used to analyse TRISO coated-particle fuel [6] and metal fuel [7], design and interpret irradiation experiments [8,9], and investigate novel fuel concepts [10].

Generally, separate codes are employed for analysing normal operation and accident reactor conditions, leading to difficulties with code coupling and code management. Developing codes able to simulate both conditions permits one to consistently account for burn-up dependent phenomena, yet requires the implementation of specific models dealing with the additional physics and increased complexity that characterize fuel rod behaviour during accident situations relative to normal operating conditions.

BISON modelling and validation results for LWR fuel rod behaviour during normal operating and power ramp conditions have been presented elsewhere, e.g., [5,11-13]. In this work, recent code developments and applications to the analysis of loss-of-coolant accidents (LOCAs) are presented. From the beginning, BISON has incorporated a large-strain mechanics formulation, essential to correctly analyse cladding ballooning during LOCAs. In order to capture the complex material

response during accident situations, however, it is also necessary to incorporate in the thermo-mechanics framework of the code specific models dealing with the high-temperature, transient phenomena involved. To this end, models for high-temperature creep, crystallographic phase transition, high-temperature steam oxidation of Zircaloy cladding and cladding failure due to burst have been recently implemented in BISON. These models are described in the first part of the present paper. Also, BISON's model of fission gas swelling and release in UO_2 has been extended to include a specific treatment of burst release effect during transients, which has been presented previously [14]. Although further extension of BISON's LOCA capability is planned, these models cover the main physical processes involved and make realistic simulations of LOCA tests possible. In the second part of the paper, we present BISON simulations of several separate effects tests of cladding ballooning and burst, as well as the Halden fuel rod LOCA test IFA-650.2.

The outline of the paper is as follows. Section 2 describes the models implemented in BISON for representing cladding behaviour during LOCAs. Section 3 presents applications of the extended BISON code to simulation of LOCA tests, and comparisons of the results to available experimental data. Conclusions are drawn in Section 4.

2. Modelling

Analysing LWR fuel rod behaviour during LOCA accidents requires accurately modelling the high temperature, transient behaviour of Zircaloy cladding. For this purpose, dedicated material models have been incorporated in the thermo-mechanics analysis framework of BISON. Models are overviewed in this section.

2.1 High-temperature cladding oxidation

The process of oxidation of Zircaloy through an exothermic reaction with the coolant affects both thermal and mechanical performance of the cladding. On the one hand, the growth of a zirconium dioxide (ZrO_2) scale on the cladding outer surface adds to the thermal resistance to heat transfer from the fuel to the coolant and leads to thinning of the metallic wall. On the other hand, oxygen uptake affects the mechanical properties (e.g., creep and resistance to burst, Section 2.4) of the zirconium alloy. Concurrent to the oxidation process, a fraction of hydrogen generated during the oxidation reaction can be absorbed into the metal, enhancing cladding embrittlement and affecting the phase transformation kinetics of the material (Section 2.2). In the high temperature range (e.g., LOCA) the coolant has become steam, and oxidation proceeds much more rapidly than at normal LWR operating temperatures. Under these conditions, the kinetics of oxide scale growth and oxygen mass gain can be described by a parabolic law, with the reaction rate constant defined as a function of the temperature through an Arrhenius relation [15]:

$$\frac{d\xi}{dt} = A \cdot \exp\left(-\frac{Q}{RT_I}\right) \tag{1}$$

where ξ is either the oxide scale thickness, $\xi=\delta$ (m), or the oxygen mass, $\xi=\chi$ (kg·m^{-2}), t (s) the time, A (m or kg·m^{-2}) the pre-exponential factor, Q (J/mol) the activation energy, R (J/mol-K) the universal gas constant, and T_I (K) the metal-oxide interface temperature. The BISON model includes correlations of this form for oxide scale growth and oxygen mass gain rates in Zircaloy-2/4, appropriate to different temperature ranges. In particular, the following approach is adopted [15]:

- For metal-oxide interface temperatures from 673 K to 1800 K, the Leistikov [16] correlation is used. The Cathcart-Pawel correlation [17] is also available and can be chosen as an option.
- Above 1900 K, the Prater-Courtright correlation [18] is used.
- Between 1800 and 1900 K, a linear interpolation is made [15].

The values for the parameters in Eq. 1 relative to the different correlations are given in Table 1. Calculation examples for temperatures of 1100 and 1950 K are illustrated in Figure 1.

For normal operating temperatures below 673 K, the EPRI/KWU/C-E oxidation model [19,20] is used in BISON.

2.2 Phase transformation of the cladding material

The increase in cladding temperature during a LOCA involves time-dependent phase transformation of Zr alloy from hexagonal (α-phase) to cubic (β-phase) crystal structure. Modelling the kinetics of crystallographic phase transformation is pivotal for the assessment of the mechanical properties essential for fuel rod integrity (deformation and burst, Sections 2.3 and 2.4). The model used by BISON calculates the evolution of the volume fraction of the new phase in Zircaloy-4 as a function of time and temperature during phase transformation in non-isothermal conditions. The model is based on [21-23]. The local phase transformation rate is expressed as

$$\frac{dy}{dt} = k(T)\left[y_s(T) - y\right] \qquad (2)$$

where y (-) is the volume fraction of β-phase, t (s) the time, y_s (-) the equilibrium value of y, and k (s^{-1}) the rate parameter. The fraction of β-phase at equilibrium is represented by a sigmoid function of temperature

Correlation	A_δ ($m^2 s^{-1}$)	Q_δ / R (K)	A_χ ($kg \cdot m^{-2}$)	Q_χ / R (K)
Leistikov	$7.82 \cdot 10^{-6}$	20214	52.42	20962
Cathcart-Pawel	$2.25 \cdot 10^{-6}$	18062	36.22	20100
Prater-Courtright	$2.98 \cdot 10^{-3}$	28420	$3.3 \cdot 10^{3}$	26440

Table 1. Parameters of the oxide scale (δ) and mass gain (χ) correlations [15].

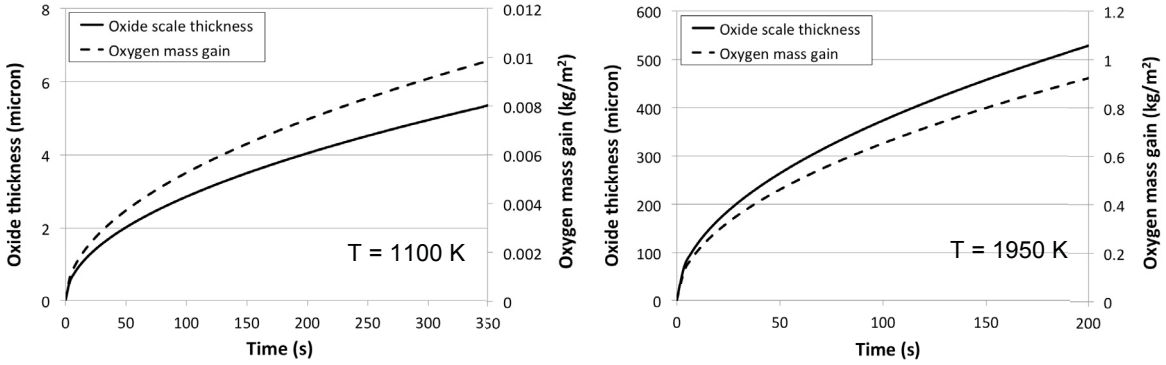

Figure 1. Oxide scale thickness and oxygen mass gain as a function of time at 1100 K (left) and 1950 K (right), calculated using the Leistikov and the Prater-Courtright correlations, respectively.

$$y_s = \frac{1}{2}\left[1+\tanh\left(\frac{T-T_{cent}}{T_{span}}\right)\right] \quad (3)$$

where T_{cent} and T_{span} are material specific parameters related to the centre and span of the mixed-phase temperature region, respectively. For Zircaloy-4, T_{cent} = 1159 − 0.096w (K) and T_{span} = 44 + 0.026w (K) [21] are used, with w being the hydrogen concentration in the range 0≤w≤1000 wppm. A model for hydrogen uptake and diffusion in the cladding has been recently developed for BISON. The model will be coupled to the present phase transformation model to provide the local hydrogen concentration, but for this work we take w=0. The rate parameter is expressed in the form

$$k = k_0 \cdot \exp\left(-\frac{E}{k_b T}\right) + k_m \quad (4)$$

where k_0 (s^{-1}) is a kinetic factor, E (J) an effective activation energy, k_b (J/K) the Boltzmann constant, and k_m (s^{-1}) a constant. For Zircaloy-4, k_0 = 60457+18129|Z| s^{-1} and E/k_b = 16650 K [21,23] are used, where Z = dT/dt is the heating rate in the range 0.1≤|Q|≤100 Ks^{-1}. The $\alpha \rightarrow \beta$ transformation is purely diffusion-controlled, while the $\beta \rightarrow \alpha$ transformation is partly martensitic. This is represented by the constant k_m given in the form [23]

$$\begin{cases} k_m = 0 & \alpha \rightarrow \beta \\ k_m = 0.2 & \beta \rightarrow \alpha \end{cases} \quad (5)$$

The starting temperatures for the onset of $\alpha \rightarrow \alpha+\beta$ and $\beta \rightarrow \alpha+\beta$ phase transformations are calculated as [21]

$$T_{\alpha\rightarrow\alpha+\beta} = \begin{cases} 1083 - 0.152w & 0 \le Z < 0.1\,Ks^{-1} \\ \left(1113 - 0.156w\right)Z^{0.0118} & 0.1 \le Z \le 100\,Ks^{-1} \end{cases} \quad (6)$$

$$T_{\alpha\rightarrow\alpha+\beta} = \begin{cases} 1300 & -0.1 < Z < 0\,Ks^{-1} \\ 1302.8 - 8.333\left|Z\right|^{0.477} & -100 \le Z \le -0.1\,Ks^{-1} \end{cases} \quad (7)$$

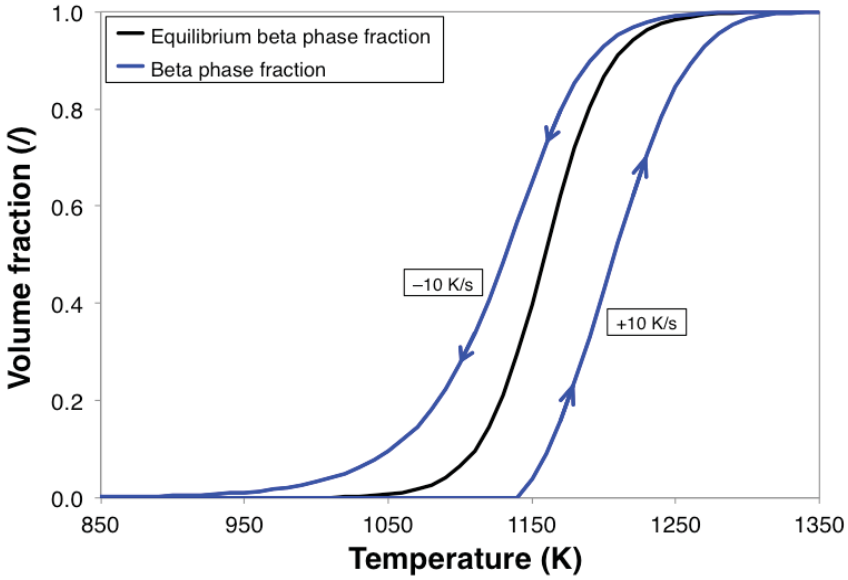

Figure 2. Calculated volume fraction of β phase as a function of temperature. Equilibrium conditions (slow temperature variation) and temperature variation rates of ±10 Ks^{-1} are considered.

for 0≤w≤1000 wppm. The calculated volume fractions of β phase as a function of temperature at equilibrium and for temperature variation rates of ±10 Ks^{-1} are illustrated in Figure 2.

2.3 High-temperature cladding creep

During a LOCA, outward creep deformation of the cladding tube under the effect of internal pressurization and high temperature drives cladding ballooning and eventual failure due to burst. In BISON, incremental nonlinear mechanical constitutive models account for elastic and inelastic strains arising from multiple phenomena at each mesh location and time step. The large creep deformation of the cladding is defined by a strain rate correlation in the form of a Norton power equation [24-26]

$$\dot{\varepsilon}_{eff} = A_{cr} \cdot \exp\left(-\frac{Q_{cr}}{RT}\right) \cdot \sigma_{eff}^{n} \tag{8}$$

where $\dot{\varepsilon}_{eff}$ (s^{-1}) is the effective strain rate, A_{cr} ($MPa^{-n}s^{-1}$) the strength coefficient, Q_{cr} (J/mol) the activation energy for the creep deformation, T (K) the temperature, σ_{eff} the effective (Von Mises) stress, and n (-) the stress exponent. The components of the strain tensor are updated in an iterative process at each time step based on the effective strain increment and a flow rule. The material parameters (Table 2) used in the model were obtained from tension tests on Zircaloy-4 tubes [25,26]. In the mixed phase (α+β) region, interpolations are made to calculate the Norton parameters. Depending on the strain rate, various approaches are adopted [25]:

- For $\dot{\varepsilon}_{eff} \leq 3 \cdot 10^{-3}$ s^{-1}, linear interpolation of ln(A), n, and Q is made between the values for pure α and middle of α+β (50%-α 50%-β) phase, and between 50%-α 50%-β and pure β phase.
- For $\dot{\varepsilon}_{eff} > 3 \cdot 10^{-3}$ s^{-1}, it is assumed that the values of ln(A), n, and Q vary linearly between the values for pure α and pure β phase.

To perform the interpolation, the fraction of each phase calculated from a dedicated model as described in Section 2.2 is used. The effective creep strain rate as a function of temperature for different stress values is illustrated in Figure 3.

2.4 Cladding burst criterion

For modelling failure due to burst of Zircaloy-4 claddings during LOCA accidents, criteria have been implemented in BISON for three different regimes:

Phase	$\dot{\varepsilon}_{eff}$ (s^{-1})	A ($MPa^{-n}s^{-1}$)	Q (J/mol)	n (-)
α	any	8737	321000 + + 24.69·(T-923.15)	5.89
50%-α 50%-β	$\leq 3 \cdot 10^{-3}$	0.24	102366	2.33
	$> 3 \cdot 10^{-3}$	Lin. Interp. ln(A)	Lin. Interp.	Lin. Interp.
β	any	7.9	141919	3.78

Table 2. Material parameters used to calculate creep of Zircaloy-4 [25,26].

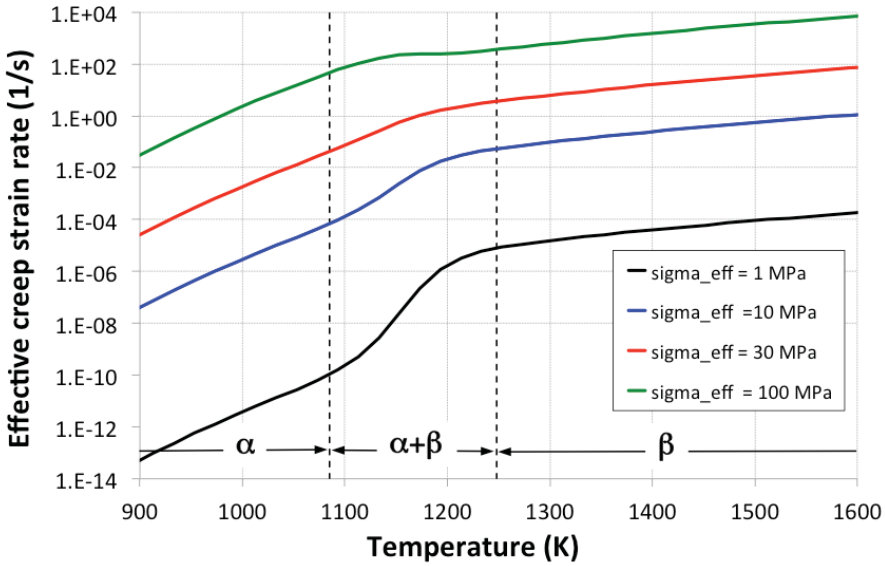

Figure. 3. Effective creep strain rate of Zircaloy-4 as a function of temperature for different values of the effective stress. The approximate temperature regions corresponding to the different crystallographic phases of the material are highlighted.

1. An overstress criterion, which assumes that the time of burst is reached when the local hoop stress equals a limiting burst stress [26]:
   $$\sigma_\vartheta \geq \sigma_b \quad (9)$$
   where σ_ϑ (MPa) is the hoop stress and σ_b (MPa) is the burst stress.
2. A plastic instability criterion, which considers cladding burst at the attainment of a limiting value for the local effective plastic strain rate [27]:
   $$\dot{\varepsilon}_{pl,eff} \geq \dot{\varepsilon}_b \quad (10)$$
   where $\dot{\varepsilon}_{pl,eff}$ is the effective plastic (creep) strain rate and $\dot{\varepsilon}_b$ is the limiting value.
3. A combination of the above criteria, which establishes that cladding burst occurs when either condition (9) or (10) is fulfilled.

The calculation of the burst stress follows the work of Erbacher et al. [26]. Based on experimental evidence, the burst stress is considered to depend on local temperature and oxygen concentration in the cladding, and is calculated as [26]:

$$\sigma_b = a \cdot \exp(-bT) \cdot \exp\left[-\left(\frac{\eta - \eta_0}{9.5 \cdot 10^{-4}}\right)^2\right] \quad (11)$$

where σ_b (MPa) is the burst stress, a (MPa) and b (K^{-1}) are constants determined experimentally, and η (-) is the oxygen weight fraction in the cladding. An oxygen weight fraction at fabrication, $\eta_0 = 1.2 \cdot 10^{-3}$, is considered [26]. The current oxygen weight fraction is computed based on the oxygen mass gain from the oxidation model (Section 2.1) as

$$\eta = \frac{2 r_{cl,o}}{\rho_{Zy} \cdot \left(r_{met,o}^2 - r_{cl,i}^2\right)} \cdot \chi + \eta_0 \quad (12)$$

where $r_{cl,o}$ (m) is the cladding outer radius, ρ_{Zy} = 6550 kg·m^{-3} the density of the cladding metal, $r_{cl,i}$ (m) the cladding inner radius, and $r_{met,o} = r_{cl,o} - \delta/R_{PB}$ with R_{PB} = 1.56 being the Pilling-Bedworth ratio for Zr.

Phase	a (MPa)	b (K^{-1})
α	830	$1 \cdot 10^{-3}$
50%-α 50%-β	3000	$3 \cdot 10^{-3}$
β	2300	$3 \cdot 10^{-3}$

Table 3: Material parameters used to calculate the burst stress [26].

The values for the parameters a and b are given in Table 3. In the mixed phase (α+β) region, linear interpolations of ln(a) and b are made between the values for pure α and middle of α+β (50%-α 50%-β) phase, and between 50%-α 50%-β and pure β phase [26]. The volume fractions of each phase are calculated by the phase transformation model described in Section 2.2.

For the limiting effective plastic strain rate, in line with [27], we choose $\dot{\varepsilon}_b = 100\ h^{-1} \approx 2.78 \cdot 10^{-2}\ s^{-1}$.

The work of Di Marcello et al. [27] showed that the criterion based purely on a limiting stress value (criterion 1) may lead to non-conservative cladding failure predictions in low-stress situations, for which a criterion including limitation of total strain or strain rate was recommended. In consideration of this, the combined criterion (criterion 3) is adopted for the simulations performed in this work and presented hereafter.

3. BISON simulations

The models described in Section 2, and their mutual interactions, have been incorporated in the thermo-mechanics framework of the BISON code. In addition, an automatic time step control based on the increment of creep strain during a time step has been implemented. Validation of the extended BISON code is ongoing, both against separate effects tests of cladding ballooning and burst as well as fuel rod LOCA tests from the Halden Reactor Project. An account of the present status of BISON validation for LOCA conditions is given hereafter. In particular, Subsections 3.1 and 3.2 deal with analyses of cladding separate effects tests, whereas Subsection 3.3 describes a first application to a Halden LOCA fuel rod test from the IFA-650 series.

3.1 REBEKA separate effects tests

3.1.1 Experiment

The REBEKA separate effects tests [26,28,29] are temperature transient tests in steam performed on single PWR-size Zircaloy-4 tubes at a variety of internal pressures and heating rates. The purpose of the tests was to establish data of cladding ballooning and burst with reference to LOCA conditions. The cladding tubes had a fabricated inner/outer diameter of 9.30/10.75 mm, with a 325 mm heated length. The cladding was heated indirectly by conduction heating from inside using an electrically insulated heater rod. The test parameters covered a range of 1 to 14 MPa for the internal rod (He) pressure and 1 to 30 K/s for the heating rate. The test atmosphere was almost stagnant steam at atmospheric pressure and 473 K. The cladding temperatures were measured by thermocouples spot-welded on the outer surface of the cladding. More details on the experimental apparatus and conditions are given in [26,28,29].

3.1.2 Calculation setup

Both 2D axisymmetric and 3D BISON models of the cladding tubes tested during the REBEKA experiments were built. For simplicity, only the heated length was modelled. The internal electric heating was simulated by a time-dependent Dirichlet temperature boundary condition applied to the tube inner wall and consistent with the experimental conditions. In particular, a parabolic temperature profile symmetric with respect to the tube mid-plane was considered, which results from the uniform axial power generation in the heater rod [29]. To estimate the temperature variation over the heated length of the cladding, simplified calculations of axial heat conduction within the rod and convection to the outer steam atmosphere were performed, based on available information on materials and experimental conditions [26,28,29]. Pressure equal to the experimental value was applied at the tube inner wall. Taking advantage of the symmetry of the problem, only the lower half of the heated cladding length was modelled. For the 3D simulations, a quarter of the cladding circumference was modelled.

3.1.3 Results

Using the 2D axisymmetric model, BISON simulations were conducted of the REBEKA experiments with a heating rate of 1 K/s, considering the full range of 1 to 14 MPa for the internal cladding pressure. The predictions of burst temperature at the various internal cladding pressures are compared to the available experimental data in Figure 4. The trend of increasing burst temperature with decreasing internal pressure is reproduced, and the quantitative accuracy of predictions is reasonable. Nevertheless, a moderate but systematic under-prediction is observed. Such discrepancies may be due to uncertainties inherent in the cladding mechanics, oxidation and phase transformation modelling, three-dimensional effects (azimuthal temperature differences) that cannot be captured by 2D modelling, as well as measurement uncertainties.

To investigate inherently three-dimensional aspects such as the effect of azimuthal temperature differences, BISON 3D simulations were conducted. For these simulations, a parabolic axial temperature profile consistent with the corresponding 2D simulation was considered. In addition, an azimuthal temperature gradient was applied. A maximum azimuthal temperature variation of 30 K

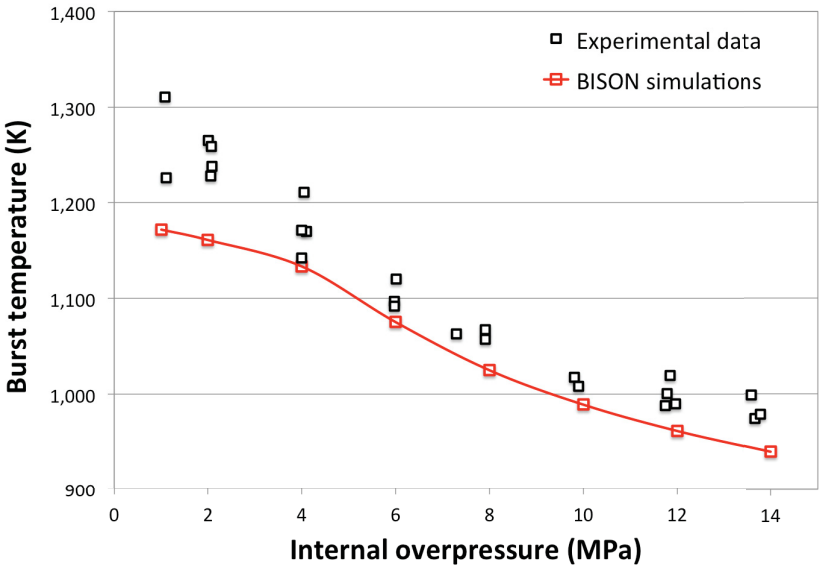

Figure 4. Comparison between BISON predictions and experimental data of cladding burst temperature for the simulations of the REBEKA tests with heating rate of 1 K/s.

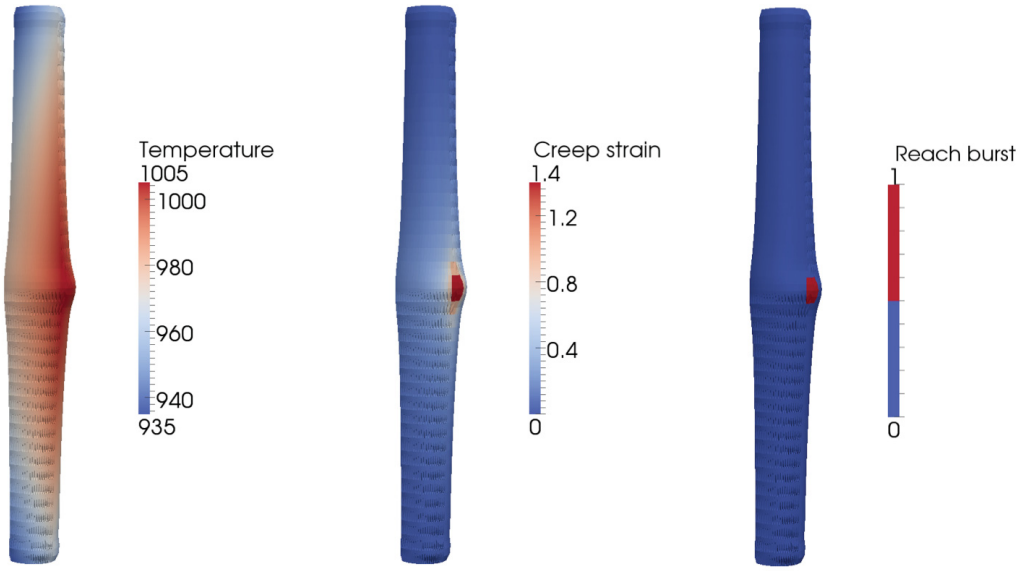

Figure 5. Contour plots for the BISON 3D simulation of the REBEKA test with 10 MPa internal pressure at the time of cladding burst. The results for the lower quarter of the heated cladding are mirrored to obtain a full-length, half circumference view. The plots are magnified 3x in the radial direction for visualization. The blur zones are due to the adopted visualization tool.

was considered, in conformity with the experimental indications from thermocouple measurements [28]. Azimuthal temperature differences are expected to play a significant role in cladding deformation and burst behaviour [26]. BISON results are presented here for the exemplifying case of 10 MPa internal pressure at the time of cladding burst. Figure 5 shows contour plots of temperature, creep strain magnitude, and locations where the local stress reached the limiting burst stress. The creep strain magnitude (-) is defined as

$$\varepsilon_{cr,mag} = \sqrt{\frac{2}{3}\mathbf{e}_{cr} : \mathbf{e}_{cr}} \tag{13}$$

where $\mathbf{e}_{cr}$ is the creep strain tensor.

The 3D simulation reproduces the non-uniform cladding ballooning and a localized burst on the hottest side of the cladding, which is consistent with experimental observations [28]. Note that the predicted burst temperature is higher (by about 10 ^{o}C) than for the corresponding 2D simulation, thus indicating that capturing 3D aspects such as the effect of azimuthal temperature differences is likely of importance for fuel analysis during LOCA accidents.

3.2 PUZRY separate effects tests

3.2.1 Experiment

Separate effects ballooning tests from AEKI [30] were performed to investigate the mechanical behaviour and strength of cladding tubes fabricated with different materials, and to provide adequate data for models validation. In particular, the PUZRY test series, which focused on Zircaloy-4 claddings, is considered in the present study. Tube samples were investigated in a resistance furnace providing isothermal conditions in the temperature range of 973-1473 K. The inner pressure of the test tube was increased linearly until the burst of the sample. The specimens

were 50 mm long with inner/outer diameters of 9.3/10.75 mm (PWR-size), respectively. The specimen was placed in a quartz test tube filled with inert gas (Ar), and heated up in an electrical furnace. The pressure of the inert gas in the quartz tube was kept at constant 0.1 MPa. After an approximately 1000 s heat-up period, the sample was pressurized with argon gas at a constant pressurization rate. Pressurization rates between $7 \cdot 10^{-4}$-$2.6 \cdot 10^{-2}$ MPa/s were tested. The effect of corrosion on the mechanical performance of Zircaloy-4 cladding was not investigated. In total, the experiment included 31 ballooning tests.

3.2.2 Calculation setup

2D axisymmetric models of the PUZRY cladding tubes were built. Heating was simulated by a Dirichlet temperature boundary condition applied to the tube outer wall, considering a 1000 s heat-up period and isothermal conditions afterwards [30]. An axial temperature gradient was considered, to allow for the temperature gradients present in the furnace [31]. The maximum temperature is applied at the mid-plane, consistent with experimental observations of localized ballooning close to the mid-plane of the specimen [30]. A maximum temperature variation of 6 ^{o}C along the specimen was considered [31]. In absence of detailed axial temperature profiles, a linear profile was adopted. Increasing pressure was applied at the tube inner wall at the experimental pressurization rate. Taking advantage of the symmetry of the problem, only the lower half of the heated cladding length was modelled.

3.2.3 Results

All 31 tests from the PUZRY series have been analysed with BISON. The predictions of tube internal pressure at burst and time to burst are compared to the experimental data from [30] in Figures 6 and 7. The accuracy of BISON analyses appears to be reasonable and in line with state-of-the-art predictions with other fuel performance codes [27].

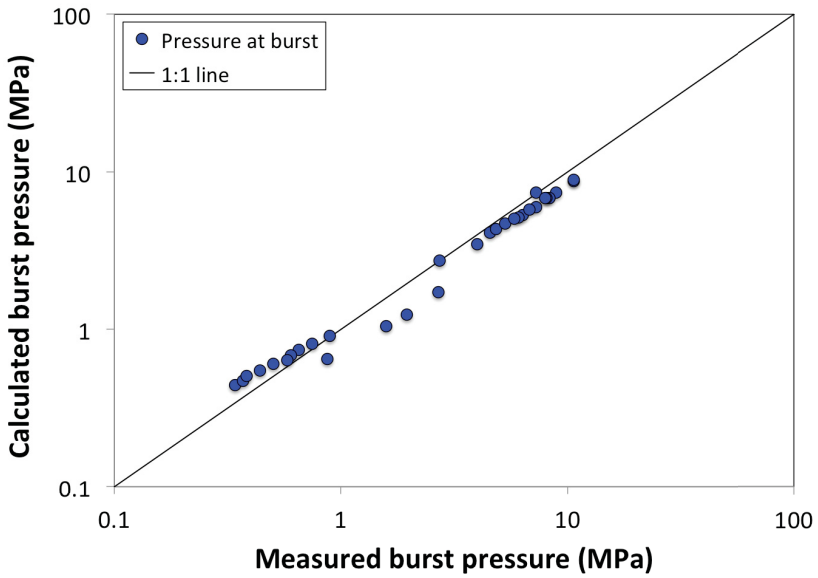

Figure 6. Comparison between BISON predictions and experimental data of cladding burst pressure for the simulations of the PUZRY tests.

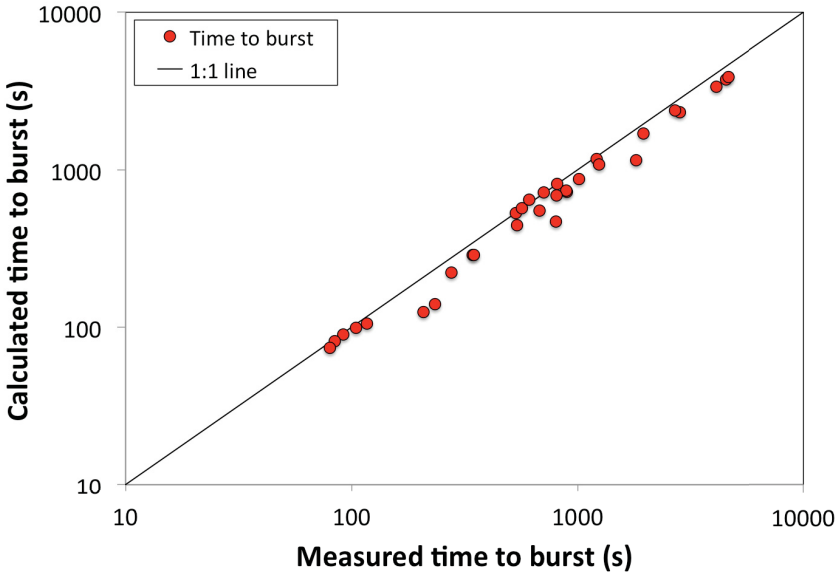

Figure 7. Comparison between BISON predictions and experimental data of time to cladding burst for the simulations of the PUZRY tests.

3.3 Fuel rod LOCA test Halden IFA-650.2

3.3.1 Experiment

LOCA tests at Halden (IFA-650 series) are integral in-pile single rod tests. Relative to separate effects tests, they also provide information on the integral behaviour of a fuel rod during a LOCA accident. The second trial test run IFA-650.2 [32,33] was performed in May 2004. The test was carried out using a fresh, pressurized PWR rod and low fission power to achieve the desired temperature conditions. The rod plenum volume was made relatively large to be able to maintain stable pressure conditions during ballooning. The fabrication characteristics of the IFA-650.2 fuel rod are reported in Table 4. The fuel rod was located in a standard high-pressure flask in the IFA-650 test rig, which was connected to a high-pressure heavy water loop and a blow-down system.

Fuel material	UO_2
Fuel density (%TD)	95.0
^{235}U enrichment (wt%)	2.0
Active stack length (mm)	500
Pellet OD (mm)	8.29
Pellet ID (mm)	0.0
Cladding material	Zy-4
Cladding ID (mm)	8.36
Cladding OD (mm)	9.50
Diametral gap (μm)	70
Free volume (cm^3)	17.4
Fill gas	He
Fill gas pressure (MPa)	4.0

Table 4. Design data of IFA-650.2 fuel rod [33].

During normal operation prior to the test, the rig was connected to the loop. Then, the rig was bypassed, and LOCA was initiated by opening the valves leading to the blowdown tank. The initial pressure in the loop was ~7 MPa and the counterpressure in the blowdown tank was ~0.2 MPa. During the LOCA phase, a low fission power of 2.3 kW/m was used to achieve the desired temperature conditions. A heater surrounding the rod was used to simulate the heat from adjacent rods. Cladding rupture occurred at ~800°C cladding temperature [32,33].

The Halden IFA-650.2 test was selected for comparative fuel performance modelling in the IAEA FUMEX-III Project [34] and is being considered also within the IAEA FUMAC Project on Fuel Modelling under Accident Conditions [35].

3.3.2 Calculation setup

A 2D BISON model of the IFA-650.2 fuel rod was constructed. Linear power and coolant pressure histories were applied consistent with the Halden experimental data. Thermal boundary conditions at the cladding outer wall were estimated in a preliminary way based on the available measured outer cladding temperatures [33]. More detailed evaluations of thermal boundary conditions for various Halden IFA-650 tests are foreseen in the frame of the FUMAC project [35] and will be considered in future work. BISON models for PWR fuel rod analysis [5,13] were adopted along with the specific LOCA models described in Section 2.

3.3.3 Results

As an initial validation of the extended BISON code against an integral fuel rod LOCA experiment, we present comparisons between calculated and experimental inner pin pressure and time to burst for the IFA-650.2 test. In Figure 8, calculated inner pin pressure is compared to the on-line experimental measurement, with predicted and experimental time to burst being also illustrated. The comparison points out that both quantities are reasonably well predicted by the extended BISON code. Rod pressure is slightly over-predicted during the heat-up phase of the test, which may be ascribed to discrepancies in the calculated plenum temperature and/or evolution of fuel rod

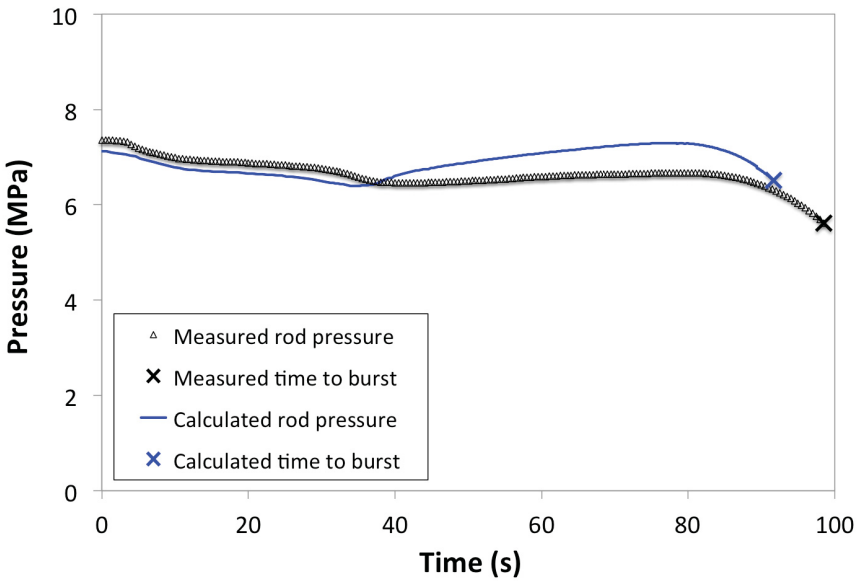

Figure 8. Comparison between measured and calculated fuel rod inner pressure and time to cladding bust for the Halden IFA-650.2 test. Time zero corresponds to the beginning of the LOCA phase.

inner volume during ballooning. Fission gas release is very low due to the test being performed with a fresh fuel rod and is not expected to affect rod pressure significantly. Calculated time to burst is within 7 s of the experimental result. These comparisons indicate an encouraging predictive capability of BISON with the interactive models dealing with cladding high-temperature behaviour and burst.

4. Conclusions

In this paper, recent developments and applications of INL's performance code BISON to the analysis of LWR fuel rod behaviour during LOCA accidents were presented. In the first part of the paper, BISON models were described for the behaviour of the Zircaloy cladding under LOCA conditions, including high-temperature steam oxidation, crystallographic phase transition, creep deformation leading to ballooning, and failure due to burst. In the second part, applications of the extended code to the analysis of LOCA experiments were presented. Analysed experiments included separate effects tests of cladding ballooning and burst, as well as the Halden IFA-650.2 fuel rod LOCA test. BISON predictions were compared to experimental data of cladding burst temperature, pressure and time for separate effects tests, as well as fuel rod inner pressure evolution and time to burst for the IFA-650.2 fuel rod test. The results indicated an encouraging predictive accuracy in view of further development and validation of the code for LOCA fuel behaviour analysis. In addition, BISON three-dimensional simulations were carried out, which demonstrated the capability to reproduce the effect of azimuthal cladding temperature variations.

Future BISON developments for the analysis of fuel rod behaviour during LOCAs will focus on several modelling aspects, including cladding oxidation coupled to wall thinning during oxide layer growth, phase transformation coupled to hydrogen uptake and diffusion, and the anisotropic creep behaviour of Zircaloy. Extension of the code validation base is also foreseen, which will involve further analyses of LOCA experiments selected within the FUMAC project, including other Halden tests from the IFA-650 series.

5. Acknowledgments

The authors wish to thank Dr. Lars O. Jernkvist (Quantum Technologies AB) for the interesting discussions about the assessment of fuel rod thermal boundary conditions, and Dr. Wolfgang Wiesenack (IFE–Halden) for information and discussions about the IFA-650 tests.

This work was funded by the INL Laboratory Directed Research and Development (LDRD) program. The manuscript has been authored by a contractor of the U.S. Government under Contract DE-AC07-05ID14517. Accordingly, the U.S. Government retains a non-exclusive, royalty free license to publish or reproduce the published form of this contribution, or allow others to do so, for U.S. Government purposes.

6. References

[1] K. Lassmann, "The Structure of Fuel Element Codes", Nuclear Engineering and Design, Vol. 57, pp. 17-39, 1980.

[2] C. Calvin and D. Nowak, "High Performance Computing in Nuclear Engineering", in: *Handbook of Nuclear Engineering*, Vol. 12, pp. 1449-1517, D.G. Cacuci, Ed., Springer Science + Business Media, LLC., New York, NY, USA, 2010.

[3] S. Bragg-Sitton, L. Ott, K. Robb, M. Farmer, M. Billone, R. Montgomery, C. Stanek, M. Todosow, and N. Brown, Technical Report INL/EXT-13-30226, Idaho National Laboratory, ID, USA, 2014.

[4] S.J. Zinkle, K.A. Terrani, J.C. Gehin, L.J. Ott, and L.L. Snead, “Accident Tolerant Fuels for LWRs: A Perspective”, Journal of Nuclear Materials, Vol. 448, pp. 374-379, 2012.

[5] R.L. Williamson, J.D. Hales, S.R. Novascone, M.R. Tonks, D.R. Gaston, C.J. Permann, D. Andrs, and R.C. Martineau, “Multidimensional Multiphysics Simulation of Nuclear Fuel Behavior, Journal of Nuclear Materials, Vol. 423, pp. 149-163, 2012.

[6] J.D. Hales, R.L. Williamson, S.R. Novascone, D.M. Perez, B.W. Spencer, and G. Pastore, “Multidimensional Multiphysics Simulation of TRISO Particle Fuel” Journal of Nuclear Materials, Vol. 443, pp. 531-543, 2013.

[7] P. Medvedev, Technical Report INL/EXT-12-27183 Revision 1, Idaho National Laboratory, ID, USA, 2012.

[8] P. Medvedev, Technical Report INL/EXT-13-30006, Idaho National Laboratory, ID, USA, 2013.

[9] A. Casagranda, , B.W. Spencer, G. Pastore, S. R. Novascone, J. D. Hales, R. L. Williamson, and R. C. Martineau, “Determination of Experimental Fuel Rod Parameters using 3D Modelling of PCMI with MPS Defects”, submitted to Enlarged Halden Programme Group Meeting, Sandefjord, Norway, May 8-13, 2016.

[10] J.D. Hales and K.A. Gamble, “Preliminary Evaluation of FeCrAl Cladding and U-Si Fuel for Accident Tolerant Fuel Concepts”, Proc. of the Water Reactor Fuel Performance Meeting – Top Fuel, Zurich, Switzerland, September 13-17, 2015.

[11] D.M. Perez, R.L. Williamson, S.R. Novascone, T.K. Larson, J.D. Hales, B.W. Spencer, and G. Pastore, “An evaluation of the nuclear fuel performance code BISON”, Proc. of the International Conference on Mathematics and Computational Methods Applied to Nuclear Science and Engineering – M&C 2013, Sun Valley, ID, USA, May 5-9, 2013.

[12] G. Pastore, L.P. Swiler, J.D. Hales, S.R. Novascone, D.M. Perez, B.W. Spencer, L. Luzzi, P. Van Uffelen, and R.L. Williamson, “Uncertainty and Sensitivity Analysis of Fission Gas Behavior In Engineering-Scale Fuel Modeling”, Journal of Nuclear Materials, Vol. 456, pp. 398-408, 2015.

[13] R.L. Williamson, K.A. Gamble, D.M. Perez, S.R. Novascone, G.Pastore, R.J. Gardner, and J.D. Hales, “Validating the BISON Fuel Performance Code to Integral LWR Experiments”, Nuclear Engineering and Design, 2016, in press.

[14] G. Pastore, D. Pizzocri, J. D. Hales, S. R. Novascone, D. M. Perez, B. W. Spencer, R.L. Williamson, P. Van Uffelen, and L. Luzzi, “Modelling of transient fission gas behaviour in oxide fuel and application to the BISON code”, Enlarged Halden Programme Group Meeting, Røros, Norway, September 7-12, 2014.

[15] G. Schanz, Technical Report FZKA 6827, SAM-COLOSS-P043, Forschungszentrum Karlsruhe, Karlsruhe, Germany, 2003.

[16] S. Leistikow, G. Schanz, H.v. Berg, and A.E. Aly, “Comprehensive presentation of extended Zircaloy-4/steam oxidation results 600-1600 C”, Proc. of CSNI/IAEA specialists meeting on

water reactor fuel safety and fission product release in off-normal and accident conditions, Risø National Laboratory, Denmark, 1983.

[17] J.V. Cathcart, R.E. Pawel, R.A. McKee, R.E. Druschel, G.J. Yurek, J.J. Campbell, and S.H. Jury, Technical Report ORNL/NUREG-17, Oak Ridge National Laboratory, TN, USA, 1977.

[18] J.T. Prater and E.L. Courtright, Technical Report NUREG/CR-4889, PNL-6166, 1987.

[19] F. Garzarolli, W. Jung, H. Schoenfeld, A.M. Garde, G.W. Parry, and P.G. Smerd, Technical Report EPRI-NP 2789, Electric Power Research Institute, Palo Alto, CA, USA, 1982.

[20] F. Garzarolli and M. Garzarolli, "PWR Zr alloy cladding water side corrosion – State of Knowledge on In-PWR Corrosion Analysis Methods of Measured Oxide Data and Oxide Thickness Prediction", Advanced Nuclear Technology International, Mölnlycke, Sweden, 2012.

[21] A.R. Massih, '"Transformation Kinetics of Zirconium Alloys under Non-Isothermal Conditions", Journal of Nuclear Materials, Vol. 384, pp. 330-335, 2009.

[22] A.R. Massih and L.O. Jernkvist, "Transformation Kinetics of Alloys under Non-Isothermal Conditions", Modelling and Simulation in Materials Science and Engineering, Vol. 17, No. 5, 2009.

[23] A.R. Massih, Technical Report TR11-008V1, Quantum Technologies AB, Sweden, 2011.

[24] P. Van Uffelen, C. Győri, A. Schubert, J. van de Laar, Z. Hózer, and G. Spykman, "Extending the Application Range of a Fuel Performance Code from Normal Operating to Design Basis Accident Conditions", Journal of Nuclear Materials, Vol. 383, pp. 137-143, 2008.

[25] H.J. Neitzel and H.E. Rosinger, Technical Report KfK 2893, Kernforschungszentrum Karlsruhe, Germany, 1980.

[26] F.J. Erbacher, H.J. Neitzel, H. Rosinger, H. Schmidt, and K. Wiehr, "Burst criterion of Zircaloy Fuel Claddings in a Loss-Of-Coolant Accident", Zirconium in the Nuclear Industry, Fifth Conference, ASTM STP 754, D.G. Franklin, Ed., American Society for Testing and Materials, pp. 271-283, 1982.

[27] V. Di Marcello, A. Schubert, J. van de Laar, and P. Van Uffelen, "The TRANSURANUS Mechanical Model for Large Strain Analysis", Nuclear Engineering and Design, Vol. 276, pp. 19–29, 2014.

[28] M.E. Markiewicz and F.J. Erbacher, Technical Report KfK 4343, Kernforschungszentrum Karlsruhe, Germany, 1988.

[29] F.J. Erbacher, H.J. Neitzel, and K. Wiehr, Technical Report KfK 4781, Kernforschungszentrum Karlsruhe, Germany, 1990.

[30] E. Perez-Feró, Z. Hózer, T. Novotny, G. Kracz, M. Horváth, I. Nagy, A. Vimi, A. Pintér-Csordás, Cs. Győri, L. Matus, L. Vasáros, P. Windberg, and L. Maróti, Technical Report EK-FRL-2012-255-01/02, Center for Energy Research, Hungarian Academy of Sciences, Budapest, Hungary, 2013.

[31] K. Kulacsy, Communication within the IAEA Fuel Modelling under Accident Conditions (FUMAC) Project, 2015.

[32] E. Kolstad, W.Wiesenack, and V. Grismanovs, “LOCA Testing at Halden, Second in-pile test in IFA-650.2”, Technical Report IFE/HR/E-2004/027, Presented at the Nuclear Safety Research Conference, Washington, DC, USA, October 25-27, 2004.

[33] M. Ek, *LOCA Testing at Halden; The Second Experiment IFA-650.2*, Technical Report HWR-813, OECD Halden Reactor Project, 2005.

[34] *Improvement of Computer Codes used for Fuel Behaviour Simulations (FUMEX-III)*, Technical Report IAEA-TECDOC-1697, 2013.

[35] J. Zhang and M. Veshchunov, “Status Update of the IAEA FUMAC Project”, Presented at the OECD/NEA Expert Group on Reactor Fuel Performance (EGRFP), Paris, France, February 16, 2016.